Investigation into Global Equivalence Ratio and External Plumes from Timber Lined Compartments

Kanellopoulos G.*, Bartlett A., Law A.

School of Engineering, The University of Edinburgh, Edinburgh, Scotland, UK
**Corresponding author's email: g.kanellopoulos@ed.ac.uk*

ABSTRACT

The construction industry promotes the use of cross-laminated timber (CLT) as a more sustainable and architectural material. This introduces unknown fire hazards in the built environment. The current study investigates the differences in the external plume between compartments with CLT surfaces and non-combustible surfaces. An exposed timber structure increases the fuel load, which in turn increases the produced flammable gases. As oxygen supply is limited by the opening, part of the flaming combustion will take place outside. This results in an external plume that could affect an adjacent building and the building of origin. The global equivalence ratio (GER) indicates how much unburnt fuel exits from the compartment opening. The GER is calculated from the air inflow rate, the stoichiometric fuel-air ratio, and the burning rate. Medium-scale experiments, with a 0.7 m cubic compartment, have been implemented to investigate the effect of exposed timber on the external plume. It was found that GER was higher when timber lining were exposed, and that this resulted in higher heat fluxes on the façade above the compartment opening.

KEYWORDS: Cross-laminated timber, compartment fire dynamics, external plume, global equivalence ratio.

NOMENCLATURE

A	Area (m^2)
f_{ex}	Excess fuel factor (-)
H	Window height (m)
$\dot{m}_a$	Mass air inflow (kg/s)
$\dot{m}_f$	Fuel mass loss rate (kg/s)
$\dot{q}''$	Heat flux (kW/m^2)
$\dot{Q}$	Heat release rate (kW)
r	Stoichiometric ratio (-)

Greek

ρ	Air density (kg/m^3)
φ_p	Global equivalence ratio (-)

Subscripts

af	Air to fuel
fa	Fuel to air
t	Internal total surface excluding floor and openings
w	Total opening surface

INTRODUCTION

Around the world, the construction industry is increasingly promoting more sustainable materials such as timber. As a consequence, cross-laminated timber (CLT) has recently become more commonplace in new mid- and high-rise buildings [1] (e.g. Canada, Norway, United Kingdom, Australia). Despite the perceived advantages in aesthetics and sustainability presented by using timber, the material also introduces unknown fire hazards into the built environment. The current

Proceedings of the Ninth International Seminar on Fire and Explosion Hazards (ISFEH9), pp. 469-478
Edited by Snegirev A., Liu N.A., Tamanini F., Bradley D., Molkov V., and Chaumeix N.
Published by St. Petersburg Polytechnic University Press
ISBN: 978-5-7422-6496-5 DOI: 10.18720/spbpu/2/k19-68

study aims to build on previous work investigating differences in the external fire plume between compartments with non-combustible surfaces and CLT surfaces [2]; and using the global equivalence ratio (GER) as an indicator of unburnt fuel exiting the compartment (e.g. [3]).

BACKGROUND

Exposed timber surfaces introduce more fuel into a compartment; the additional area of the fuel also increases the rate of production of flammable gases. Combustion in a compartment is limited and controlled by oxygen entering through any openings. The rest of the combustion process takes place outside the compartment; this leads to flaming in the external plume. The external plume has the potential to affect the spread to the adjacent buildings, mostly by radiation [4], and onto the building of origin by convection and radiation.

Fuel

Bullen [5] demonstrated that increasing the fuel area in a compartment fire results in an increase of the excess fuel factor; this means that more fuel is burnt outside the compartment. Drysdale [6] gives excess fuel factor as:

$$f_{ex} = 1 - \dot{m}_a \big/ \left(r_{af} \dot{m}_f \right) . \tag{1}$$

An alternative way to express the idea of excess fuel factor is using the global equivalence ratio [7]. This ratio indicates how much unburnt fuel exits from the compartment opening. In this context, the ratio is indicative in that, under the assumptions of infinitely fast mixing and stoichiometric burning, a GER of unity means that there is sufficient oxygen within the compartment to burn all available pyrolysate; a value of zero translates to no burning; values higher than unity indicate the amount of unburnt fuel leaving the compartment. Knowledge of GER is therefore part of the information needed to understand the potential for external flaming and the impact of this on the overall behaviour of the external plume, and potential for fire spread. The GER is calculated by Eq. (2).

$$\varphi_p = \dot{m}_f \big/ \left(\dot{m}_a r_{fa} \right) , \tag{2}$$

where $\dot{m}_f$ is the mass loss rate, $\dot{m}_a$ is the air inflow rate in the compartment, and r_{fa} is the stoichiometric fuel-to-air ratio (the inverse of r_{af} used for the excess fuel factor). Deriving from above, the relationship between Eq. (1) and Eq. (2) is:

$$\varphi_p = 1 \big/ \left(1 - f_{ex} \right) . \tag{3}$$

Butcher et al. [8] demonstrated that the position of combustible material can affect flaming formation in the plume. For this reason, different configurations of exposed timber surfaces are explored in this work.

Flaming in the external plume

Yokoi [9] was one of the first to study the fire hazard from hot currents exiting a compartment opening. More recently, Delichatsios et al. [10] calculated the mass of excess fuel leaving from the opening. Asimakopoulou et al. [3] calculated GER and used it as an indicator for external flaming in their scaled pool fire experiments. The present study builds on this approach to characterise the GER from timber lined compartments, and measure the resulting heat flux.

Methodology

The methodology for investigating these phenomena was to create a scaled compartment with exposed timber surfaces in different configurations. Mass loss rate, mass inflow rate, and the

resultant heat flux from the plume on the façade and opposite the opening were all quantified. Based on these measurements, GER was also calculated to allow a comparison between different configurations.

Experimental setup

A scaled compartment (Fig. 1) was constructed using 25 mm thick vermiculite boards, a material chosen because of its inert nature. The compartment internally was a 700 mm cube. The compartment was supported using steel profiles. The compartment was sealed on all joints, inner and outer, with fire cement Mapei Mapeflex Firestop 1200 °C.

The key variable of interest was the area and configuration of exposed timber, as indicated above. Three different configurations of the compartment box were examined: no exposed CLT (i.e., completely inert compartment); exposed CLT back wall; exposed CLT ceiling. Where CLT panels were used, these were 700 mm wide, 800 mm long, and 140 mm thick.

The opening was a 200 mm wide full height central slot. This gave an opening factor of 19.7 $m^{-1/2}$ – where the opening factor is defined by Thomas [5] as $A_t/(A_w H^{0.5})$, where A_t (m^2) is the internal area of the compartment excluding the floor and any openings, A_w (m^2) is the area of the openings, and H (m) is the opening height. This opening factor (and slot arrangement) was chosen based on its similarity to previous work [11, 12, 13] – and the potential to vary the opening width parametrically in future studies.

An 18 kg wooden crib (of stick thickness 38 mm) was located on the compartment floor. Based on an assumed heat of combustion of 17.5 MJ/kg, this gave a total fuel load of 315 MJ, or 643 MJ/m^2. An instrumented false "façade" was located above the compartment on the same plane as the opening. This was constructed from a 25 mm thick vermiculite board.

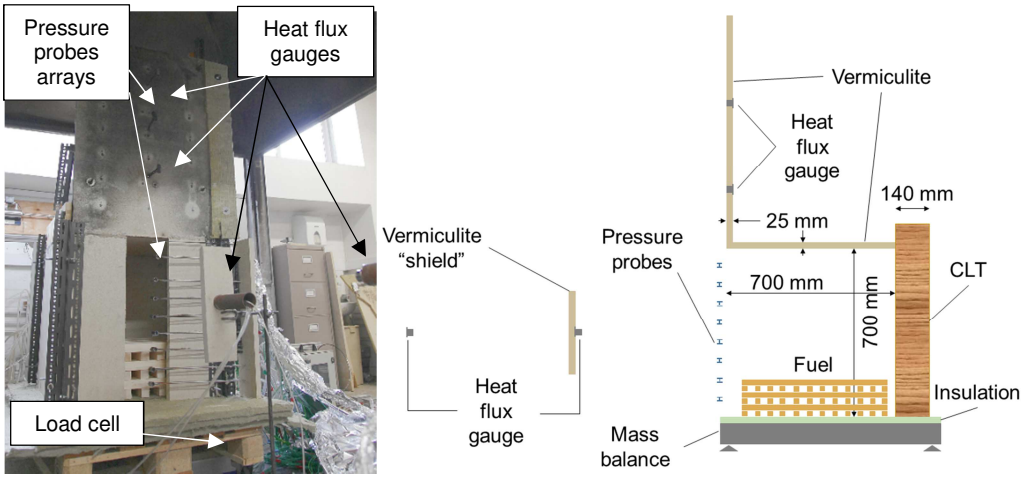

Fig. 1. (a) The experimental setup with annotations for the equipment used. (b) Indicative compartment and instrumentation geometry.

Instrumentation

The following parameters of interest were measured as described below.

- Mass loss rate, $\dot{m}_f$, was measured by placing the entire compartment assembly on a mass balance.

- Mass rate of air entering the compartment, $\dot{m}_a$, was calculated using velocity data from bi-directional pressure probes placed on the centreline of the opening. Due to limitations of the instrumentation to capture the flow profile, the number of probes used increased throughout the experimental programme for a better resolution (this is discussed further below).
- The heat flux, $\dot{q}''$, on the façade above the compartment was measured using water-cooled heat flux gauges – these were placed at 240 and 600 mm above the top of the opening.
- The heat flux, $\dot{q}''$, opposite the compartment was measured using water-cooled heat flux gauges – these were placed at 650 and 1300 mm from the compartment opening.
- Heat release rate, $\dot{Q}$, was measured using a furniture calorimeter.

A vermiculite "shield" was used to block the opening radiation to the gauge at 1300 mm, as shown in Fig. 2. The intent of this configuration was to distinguish between radiation originating from within the compartment, and that associated to the plume/external façade. Readings were made at 1 Hz.

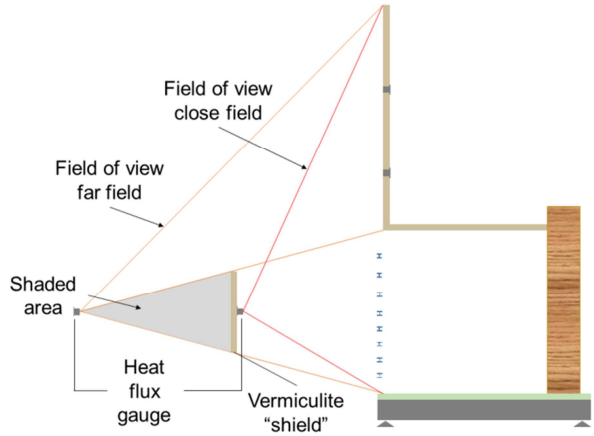

Fig. 2. Field of view of the heat flux gauges opposite the compartment.

Errors

Key sources of error, associated to each of the above parameters of interest, were identified and are presented in Table 1. The mass loss rate was measured with a mass balance of ±2 g accuracy. The air flow was measured centrally at various heights, resulting in different areas of influence for each probe; the pressure transducers used have an accuracy of ±0.25 Pa; the pressure reading was converted to velocity using the Bernoulli equation. The heat flux gauges used have a sensitivity of ±0.008 mV/(kW/m^2).

The heat release rate measurements have errors regarding the gas analyser accuracy limitations, and the calculation method used.

No measurement was made of the oxygen consumption inside the compartment, so stoichiometric burning conditions in the compartment might not (and are, indeed, unlikely to) apply. The maximum error introduced by this assumption is +1 to the GER value, meaning that no fuel is being consumed in the compartment. This can be identified and visually contradicted.

RESULTS

Key data are recorded in Table 1. It is notable from this information that the time to cessation of external flaming was approximately 10-15 minutes longer for compartments with CLT linings than for the inert compartments. It is also notable that the maximum heat release rate and measured maximum heat fluxes were higher for the CLT lined compartments.

Table 1. Significant observations from the experiments

	Inert		Back wall		Ceiling	
	1	2	1	2	1	2
Time to external flaming	1:31	1:23	0:49	1:24	1:10	1:38
Time to cease external flaming[a]	33:00	31:00	41:00	42:00	48:00	46:00
Peak HRR (kW)	165	184	214	190	218	195
Average HRR (kW)[b]	140	150	165	170	170	170
Total heat released (MJ)	4.48	4.89	5.92	5.70	6.31	5.86
Total mass loss (kg)	19.92	19.18	25.25	25.46	27.11	25.84
Max heat flux 0.65 m opposite opening	12.9	13.8	15.2	12.8	15.0	14.0
Max heat flux 0.24 m above opening	15.8	18.9	21.1	-	24.2	26.1

[a] estimated visually to the nearest minute
[b] during approximate steady state

Fuel in the inert compartments burned out without intervention. Manual extinction was applied in all exposed timber experiments, as the fire posed a hazard to the instrumentation. In all cases, there was no external flaming in the plume at the time of extinction.

Integrating the HRR and mass loss rates, a 20-30% higher total heat release is observed in all exposed timber cases, without a clear distinction between the two different positions of the CLT.

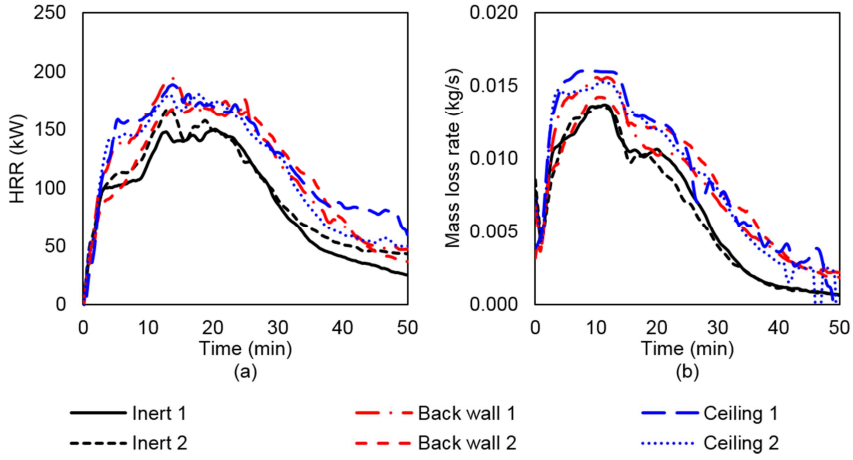

Fig. 3. (a) Heat Release Rate for each configuration, (b) Mass loss rate for each configuration.

Figure 3(a) shows higher heat release rate for the exposed timber configurations compared to the inert. It is notable that all of the experiments exhibit a two-step increase in HRR. Figure 3(b) shows

that the mass loss rate for exposed timber configurations is higher than for inert compartments. No distinction is discernable between the two different CLT configurations.

Figure 4 presents the heat fluxes as they were recorded in the two different locations, opposite the compartment and on the façade. A 100-point LOESS smoothing function was applied in all measurements.

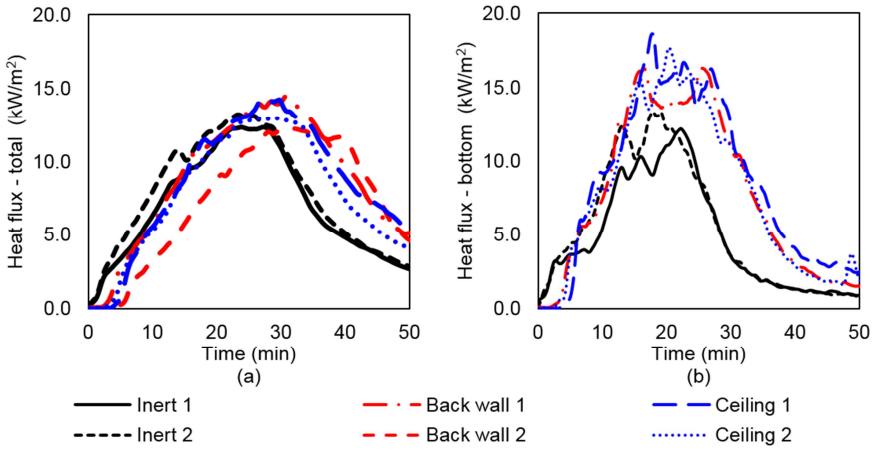

Fig. 4. (a) Heat flux opposite the compartment at 650 mm. (b) Heat flux on the façade measured at 240 mm height above the top of the opening.

The inert compartments produced lower irradiance than the timber lined ones as a whole and in terms of just the plume. Measurements from the second exposed back wall experiment are not available due to instrumentation failure. Higher heat fluxes were recorded from the plume of the lined compartments. The average value on the lower heat flux gauge in the case of the vermiculite compartments was 11 kW/m^2 and the timber lined values was 15 kW/m^2.

Based on the results presented in Fig. 4(a) and Fig. 4(b), a clear differentiation cannot be made between the heat flux from CLT back wall or ceiling configurations. Nevertheless, higher heat fluxes have consistently been observed from the CLT lined compartments in comparison to compartments with inert wall linings.

Analysis

Mass inflow

Due to the sensitivity of the differential pressure transducers, an inherent uncertainty existed in the low-velocity inflow measurements; less of an uncertainty was in the outflow due to higher velocities.

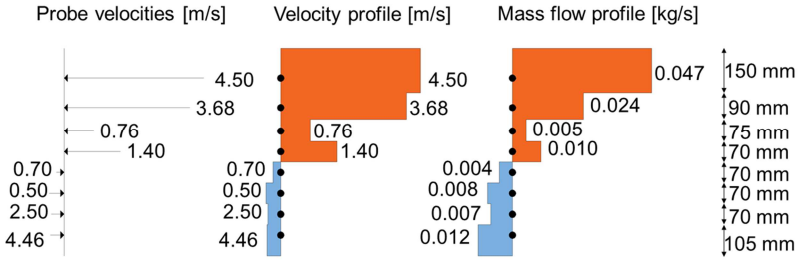

Fig. 5. (from left to right) Pressure probe velocity measurements. Assumed velocity profile in the calculations. Mass flow profile.

An additional error was introduced to the mass inflow rate calculation due to the assumption that air velocity is the same in the area of influence of each probe. Figure 5 shows an example flow profile from the second exposed back wall experiment at 17:00 minutes. Individual readings were associated with an appropriate area of the opening, and these were converted to mass flow readings based on the density of gas (thermocouple measurements were made in the same location as the bi-directional probes).

It was found (unsurprisingly) that the flow rates in were substantially lower than the flow rates out. As a consequence the relative error for the mass inflow, was greater than for the outflow. This error is illustrated in Fig. 6(a). Due to the high error associated with the mass inflow readings, an alternative (more accurate) value for mass inflow was obtained based on the outflow minus the mass burning rate. The resulting mass flow rates based on this calculation technique are plotted in Fig. 6(b). Also plotted for reference is the classical solution for mass flow in $0.5A_wH^{0.5}$.

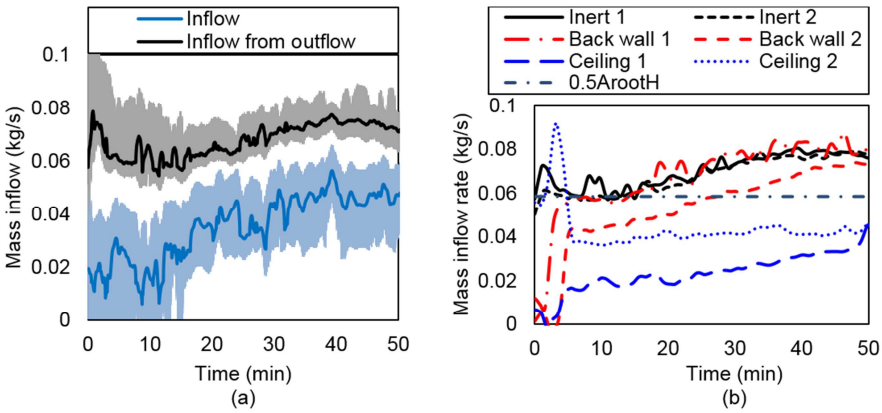

Fig. 6. (a) Error comparison of inflow rate estimation techniques (inert compartment). (b) Mass inflow rate for each configuration.

Inflow data from the first exposed ceiling seem to be substantially lower compared to the rest of the cases. Closer examination of the pressure measurements indicates that one probe reading appeared to be erroneous (i.e., it did not follow the expected flow profile). This indicates an error in capturing valid flow measurements, as the rest of the data acquired from the experiment seem to be comparable to the information from the second exposed ceiling experiment. The authors decided to disregard inflow values from Ceiling 1.

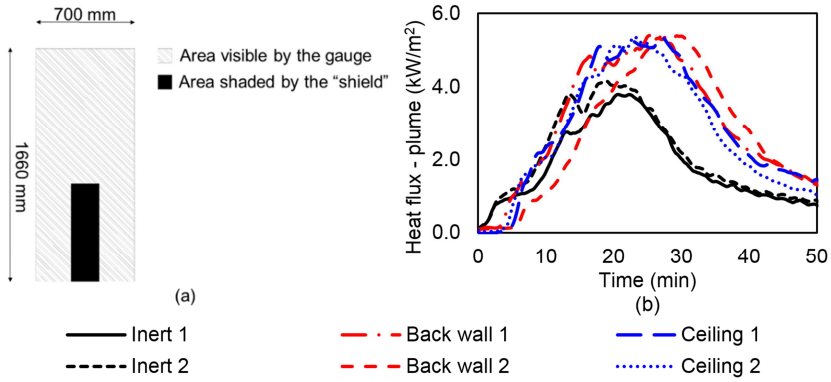

Fig. 7. (a) Front view of the area of the compartment visible by the heat flux gauge at 1300 mm. (b) Heat flux opposite the compartment excluding the opening at 650 mm.

Measurements of heat flux opposite the opening were made at different distances from the center of the opening plane. The relative contribution of radiation from within the compartment and associated to the plume can be found by applying a configuration factor to the data. The calculated configuration factor for the striped area of Fig. 7(a) at 1300 mm was 0.118, based on McGuire's work [14]; this excludes radiation from the opening. The configuration factor at 650 mm for the non-shielded area was 0.272.

This calculation allows a comparison between the total heat flux and the heat flux only from the plume to be made. The peak and average values for each case are shown in Table 2. Steady-state times for the whole compartment and the plume appear to differ in most cases. The plume had one third of the irradiance of the whole burning compartment.

Table 2. Key heat flux comparison for the whole compartment and the plume

		Inert		Back wall		Ceiling	
		1	2	1	2	1	2
Whole compartment	Peak heat flux (kW/m^2)	12.9	13.8	15.2	12.8	15.0	14.0
	Average heat flux (kW/m^2)	12.3	12.8	13.9	11.9	13.4	12.7
	Steady state time (s)	360	520	560	720	770	720
Plume	Peak heat flux (kW/m^2)	4.2	4.7	6.0	6.0	5.8	5.7
	Average heat flux (kW/m^2)	3.5	3.8	4.9	4.3	5.1	4.9
	Steady state time (s)	600	600	930	930	700	700

Given the uncertainty associated with the mass inflow calculations, GER was calculated using two methods. Firstly the mass-flow-in was defined based on the measured data, secondly it was assumed constant based on the classical value of $0.5A_w H^{0.5}$ (giving 0.059 kg/s). GER from these two methods is shown in Figs. 8 (a) and (b). Key observations from these data are as follows:

- A comparison of the calculated GER with the times of observed external flaming (given in Table 1) indicates that even when GER<1, there is some external flaming.
- CLT lined compartments give a higher overall GER than inert compartments.
- Both methods used to calculate GER (measured inflow and inflow from the classical theory) demonstrate that a difference between exposed CLT ceiling and back wall configurations is not discernible.

The maximum GER values (from inflow measurements) were 1.44, 1.37, 1.64, 1.64, 1.66 for Inert 1, Inert 2, Back wall 1, Back wall 2, Ceiling 2, respectively. For the classical theory inflow data, the peak values were 1.30, 1.29, 1.48, 1.35, 1.45, respectively, and for Ceiling 1 it was 1.52.

Figures 8 (c) and (d) show the heat flux on the façade as a function of GER. It is notable that the peak heat flux does not coincide with the peak GER value. Furthermore, it is notable that a hysteresis "loop" is forming whereby the relationship between GER and heat flux is different during the growth/steady-state, and decay of the fire. This indicates that in a dynamic scenario the maximum heat flux cannot be plotted only as a function of GER. It is observed from this analysis that the inert compartments form a smaller "loop" than the compartments with CLT linings.

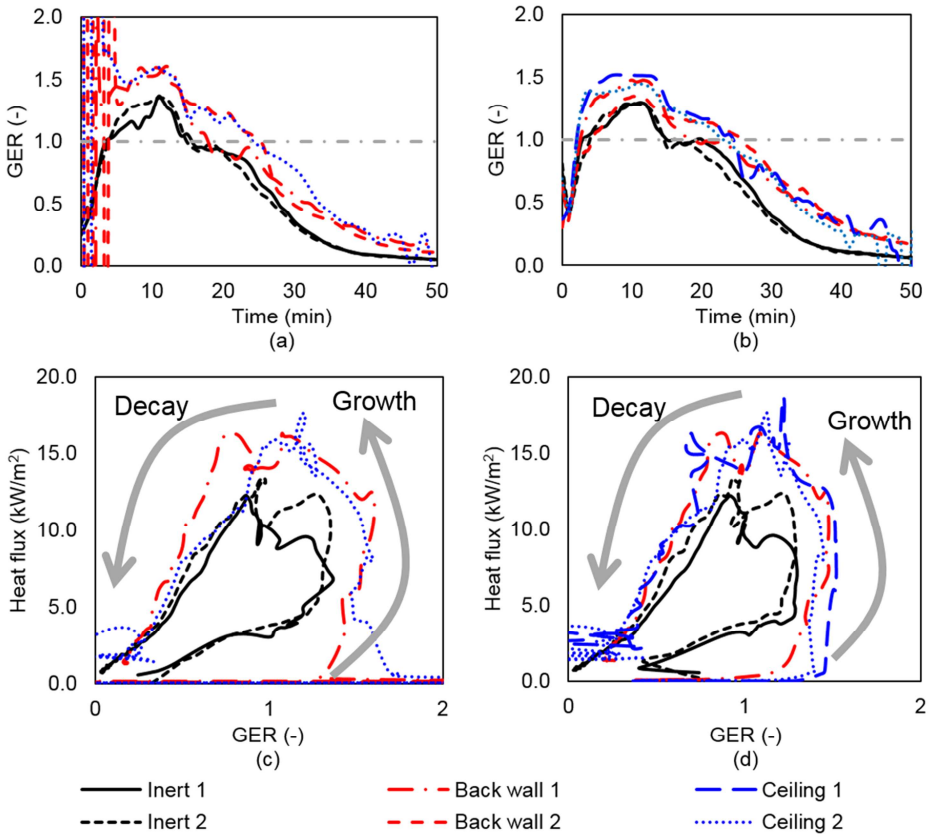

Fig. 8. (a) GER using inflow data. (b) GER using $0.5A_wH^{0.5}$. (c) Heat flux on the façade vs. GER (inflow). (d) Heat flux on the façade vs. GER ($0.5A_wH^{0.5}$)

CONCLUSION

A series of experiments of compartment fires was carried out in order to quantify GER for inert and timber lined compartments, and to measure the resulting heat flux on the façade above the compartment, and directly opposite the compartment. It was found that, when compared against compartments with inert linings, compartments with exposed timber linings have prolonged external flaming resulting in a greater GER, and induce greater heat fluxes above the opening and opposite the opening.

In terms of GER, or induced heat flux, it was not possible to distinguish between compartments with and exposed CLT ceiling and those with an exposed CLT back wall. It was found that the relationship between GER and induced heat flux opposite/above the compartment was substantially influenced by the stage of the fire.

Further investigation is suggested to distinguish the two cases in a more reliable manner and better relate excess fuel leaving a compartment to the behaviour of the external plume.

ACKNOWLEDGEMENTS

The authors would like to acknowledge EPSRC for their support of this work under the grant “Fire Spread from Mass Timber Buildings” (grant number EP/R012296/1).

REFERENCES

[1] F. Mills, Top 5: The World's Tallest Timber Buildings, The B1M, 2017. [Online]. Available: https://www.theb1m.com/video/top-5-the-world-s-tallest-timber-buildings. [Accessed: 15-Jun-2018].

[2] C.G. Putynska, A. Law, J.L. Torero, An investigation into the effect of exposed timber on thermal load, In: 24th Australasian Conference on the Mechanics of Structures and Materials, 2016, pp. 939–944.

[3] E.K. Asimakopoulou, D.I. Kolaitis, M.A. Founti, Thermal characteristics of externally venting flames and their effect on the exposed façade surface, Fire Saf. J. 91 (2017) 451–460.

[4] M. Law, Heat Radiation from Fires and Building Separation, Borehamwood, UK, 1963.

[5] M.L. Bullen, P.H. Thomas, Compartment fires with non-cellulosic fuels, Proc. Combust. Inst. 17 (1979) 1139–1148.

[6] D. Drysdale, An introduction to fire dynamics, Third ed., John Wiley & Sons, Ltd., 2011.

[7] D. Gottuk, B. Lattimer, Effect of Combustion Conditions on Species Production, In: SFPE Handbook of Fire Safety Engineering, Fifth Ed., M. Hurley, Ed., New York, 2016, pp. 486–528.

[8] E.G. Butcher, G.K. Bedford, P.J. Fardell, Further experiments on temperatures reached by steel in building fires, In: Joint Fire Research Organisation Symposium No. 2, 1968, pp. 2–17.

[9] S. Yokoi, Study on the prevention of fire-spread caused by hot upward current, Tokyo, Japan, 1960.

[10] M.A. Delichatsios, G.W.H. Silcock, X. Liu, M. Delichatsios, Y.P. Lee, Mass pyrolysis rates and excess pyrolysate in fully developed enclosure fires, Fire Saf. J. 39 (2004) 1–21.

[11] R.M. Hadden, A.I. Bartlett, J.P. Hidalgo, S. Santamaria, F. Wiesner, L.A. Bisby, S. Deeny, B. Lane, Effects of exposed cross laminated timber on compartment fire dynamics, Fire Saf. J. 91 (2017) 480–489.

[12] C.J. Bateman, A.I. Bartlett, L. Rutkauskas, R.M. Hadden, Effects of Fuel Load and Exposed CLT Surface Configuration in Reduced-Scale Compartments, In: 2018 World Conference on Timber Engineering, 2018.

[13] P.H. Thomas, A.J.M. Heselden, Supplementary reports of work for the CIB international co-operative research programme on fully-developed fires, Fire Res. Note, no. 923, 1972.

[14] J.H. McGuire, The Calculation of Heat Transfer by Radiation, Fire Res. Notes, no. 20, 1952.